

1 This is the author's final version of the manuscript published in
2 [Remote Sensing of Environment 156 \(2015\) 96–108](#).
3 The original publication is available at www.elsevier.com/locate/rse, [doi:10.1016/j.rse.2014.09.018](https://doi.org/10.1016/j.rse.2014.09.018)
4

5 Introduction to GlobSnow Snow Extent products with considerations for
6 accuracy assessment
7

8 Authors:

9 Sari Metsämäki, Finnish Environment Institute

10 Jouni Pulliainen, Finnish Meteorological Institute

11 Miia Salminen, Finnish Environment Institute and Finnish Meteorological Institute

12 Kari Luojus, Finnish Meteorological Institute

13 Andreas Wiesmann, Gamma Remote Sensing AG

14 Rune Solberg, Norwegian Computing Center

15 Kristin Böttcher, Finnish Environment Institute

16 Mwaba Hiltunen, Finnish Meteorological Institute

17 Elisabeth Ripper, Enveo IT GmbH
18

19 Corresponding author:

20 Sari Metsämäki, Finnish Environment Institute, sari.metsamaki@environment.fi

21 P.O.Box 140, FI-00251 Helsinki, Finland
22

23 **Abstract**

24 The European Space Agency's Data User Element (DUE) project GlobSnow was established to create
25 a global database of Snow Extent and Snow Water Equivalent. The Snow Extent (SE) product
26 portfolio provided within ESA DUE GlobSnow (2008–2014) is introduced and described, with a
27 special focus on the Daily Fractional Snow Cover (DFSC) of the SE version 2.0 and its successor 2.1
28 released in 2013–2014. The fractional snow retrieval uses the SCAMod method designed especially to
29 enable accurate snow mapping including forests. The basics of the methodology are presented, as
30 well as the cloud screening method applied in SE production. Considerations for future validations
31 together with discussion on some current issues and potential inaccuracies are presented. One focus of
32 the investigation is on the representativeness of reference FSC generated from Landsat Thematic
33 Mapper (TM) and Enhanced Thematic Mapper Plus (ETM+) data, with a particular interest in forested
34 areas. Two methods for reference data generation are investigated. When comparing the GlobSnow
35 Daily Fractional Snow Cover to these reference data, we try to identify how the comparison reflects
36 the possible inaccuracies of the DFSC and to define the conditions where the reference data are not
37 representative. It is obvious that the evaluation result strongly depends on the quality of the reference
38 data, and that the two methods investigated cannot provide representative reference data for dense
39 forests. For fully snow-covered dense conifer forest area in Finland, a Root Mean Squared Error of
40 20–30% was obtained from comparisons although DFSC indicated full snow cover correctly. These
41 first evaluations would indicate a good performance of GlobSnow SE products in forests; however,
42 this does not necessarily show up in validations due to the non-representativeness of the reference
43 data. It is also concluded that GlobSnow SE products are sensitive to the representativeness of the
44 applied SCAMod parameters and that FSC overestimations may occur in dense forests. GlobSnow SE
45 products are available at www.globsnow.info/se/.

46

47 **Keywords:** Snow extent, Fractional snow cover, ATSR-2, AATSR, forest, Northern
48 Hemisphere, GlobSnow

49

50 **1. Introduction**

51 Reliable information on seasonal, inter-annual and long-term changes in snow extent and snow mass
52 is important for climate change studies and water management (e.g. Choi et al., 2010; Gong et al.,
53 2007; Kite and Pietroniro, 1996; Schmugge et al., 2002). The two commonest snow variables detected
54 by means of Earth observation are Snow Extent (SE) – featuring binary ‘snow/non-snow’ information
55 or sub-pixel Fractional Snow Cover, FSC – and Snow Water Equivalent (SWE). Snow extent is
56 typically derived from optical remote sensing data using single or multi-band reflectance data in the
57 visible and near-infrared region, while snow water equivalent can be retrieved with passive
58 microwave techniques.

59 The European Space Agency’s Data User Element (DUE) project GlobSnow was established to
60 create a global database of Snow Extent and Snow Water Equivalent. GlobSnow-1 was launched in
61 2008 and candidates for the Climate Data Record (CDR) on SE and SWE were introduced in 2011.
62 These prototype versions were further developed in the sequel project GlobSnow-2 (2012–2014). This
63 paper introduces the current GlobSnow SE products (versions 2.0 and 2.1) with a specific focus on
64 daily product featuring fractional snow cover, and describes the methodology for FSC retrieval.

65 A very commonly used snow database is the suite of NASA MODIS (Moderate-Resolution
66 Imaging Spectroradiometer) snow products (Hall et al., 2002; Riggs et al., 2006), archived and
67 distributed by NSIDC (National Snow and Ice Data Center, US). The MODIS snow products have
68 been extensively validated by the research community (e.g. Ault et al., 2006; Hall and Riggs, 2007;
69 Huang et al., 2011; Rittger et al., 2013; Wang et al., 2008); e.g. Rittger et al. (2013) report a Root
70 Mean Squared Error (RMSE) ~23% (FSC %-units) for Collection 5 MOD10A1 fractional snow. This
71 agrees with the results by Metsämäki et al., (2012) where a comparison between Collection 5
72 MOD10_L2 fractional snow and *in situ* FSC observations in Finland resulted in an RMSE of 20%. As
73 for all currently available methods, the presence of forest canopy poses a problem for MODIS snow
74 retrievals, since the canopy obscures the sensor's view of the ground. Several methodologies have
75 been developed to better adjust to the presence of forest, but the problem remains unsolved (Hall and
76 Riggs, 2007; Klein et al., 1998; Rittger et al., 2013; Vikhamar and Solberg, 2003, Dietz et al., 2012).

77 As forests comprise vast portions of seasonally snow-covered regions of the Northern Hemisphere,
78 this is a serious issue.

79 The GlobSnow SE method development has been particularly focused on fractional snow
80 retrievals in forested areas using ESA ERS-2/ATSR-2 (Along Track Scanning Radiometer) and
81 Envisat/AATSR (Advanced Along Track Scanning Radiometer) data. Based on the evaluation of
82 three different candidate methods, the semi-empirical reflectance model-based method *SCAmod* by
83 Metsämäki et al., (2005) was chosen to be applied to plains while the linear spectral unmixing method
84 *NLR* by the Norwegian Computing Center NR (Solberg and Andersen, 1994; Solberg et al., 2006) was
85 to be applied to mountain areas (the borderline as indicated by a mountain mask). Using two different
86 methods, however, produced inconsistencies at the mountain borderlines (Solberg et al., 2011).
87 Therefore it was decided that only one method would be applied, instead of two. The *SCAmod*
88 method was found to provide approximately similar accuracy as *NLR* for mountains and non-forested
89 plains while providing a superior performance for forests, so it was chosen for application to the entire
90 geographical domain of GlobSnow. Indeed, the challenge with GlobSnow has been the expansion of
91 an (originally) regionally applied method to a hemispheric scale.

92 In the present paper we present first comparisons between GlobSnow daily fractional snow cover
93 products and snow maps generated using high resolution Landsat Thematic Mapper (TM) and
94 Enhanced Thematic Mapper Plus (ETM+) data. The aim is not to present an actual validation; instead,
95 we provide considerations for the accuracy of GlobSnow products in different land covers and how
96 this reflects on the comparison results. Particularly, the feasibility of two different methods for
97 generating reference FSC from TM/ETM+ data is evaluated. These evaluations aim at a better
98 understanding of how the validation results depend on the methodology chosen for reference data
99 generation. The findings will support future validation and intercomparison work.

100

101 **2. GlobSnow SE product overview**

102 The GlobSnow SE product portfolio includes maps of Fractional Snow Cover (FSC, range 0–100% or
103 0–1) on a 0.01°×0.01° geographical grid and they cover the Northern Hemisphere in latitudes 25°N–

104 84°N and longitudes 168W–192E. GlobSnow SE products are based on data provided by ERS-
105 2/ATSR-2 (1995–2003) and Envisat/AATSR (2002–2012), so that a continuous dataset spanning 17
106 years is obtained.

107 The ATSR-2 is a seven channel instrument providing visible and near-infrared measurements at 1
108 km spatial resolution. The ATSR-2 was successfully launched on board ESA's ERS-2 spacecraft in
109 1995 and provided data until 2008. Its successor, the AATSR started operations in March 2002 and
110 provided data until 2012. Swath width for both these sensors is only ~500 km so complete spatial
111 coverage at mid-latitudes cannot be achieved daily. The relevant bands for GlobSnow SE are Band 1
112 (0.545–0.565 μm) and Band 4 (1.58–1.64 μm) used for FSC retrievals; thermal bands 5, 6 and 7
113 centered at 3.7 μm , 10.85 μm and 12 μm , respectively, are used for cloud screening. The input ATSR-
114 2/AATSR data used for SE v2.0 production are from the ESA 3rd full reprocessing exercise, which
115 had the new datasets released during late 2013. It was found later that v2.0 SE products whenever
116 based on AATSR suffer from poor geolocation accuracy; after reprocessing, this problem is not
117 present in SE v2.1.

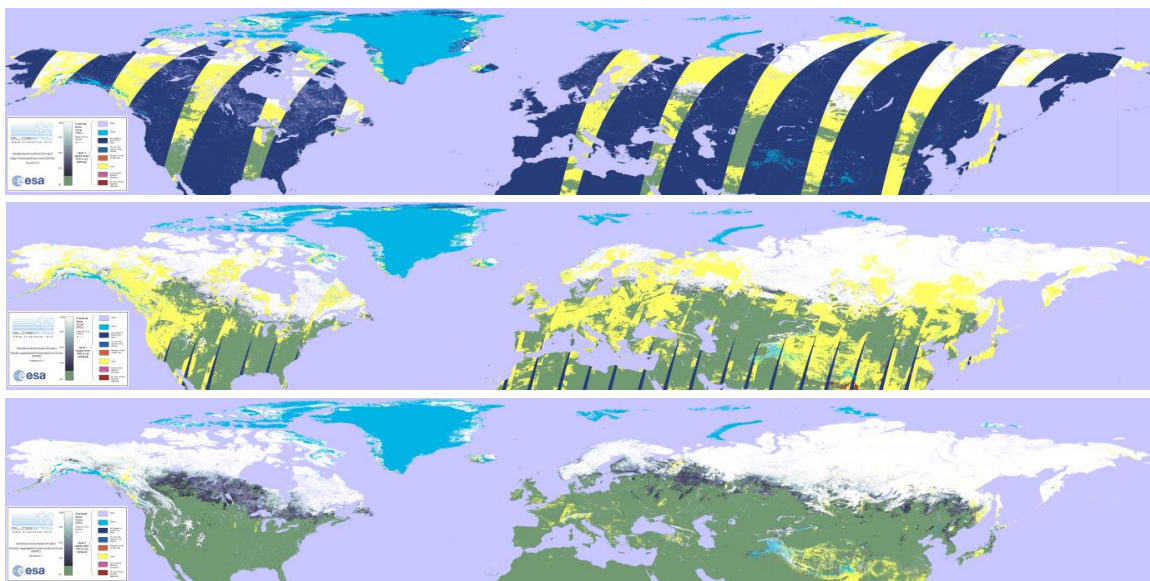
118 The GlobSnow processing system reads ESA provided Level 1B data and transfers them to the
119 GlobSnow SE latitude-longitude grid based on the geolocation grid tie points provided within the data
120 using bi-linear resampling. All orbits within the product geographical domain available within a day
121 are processed and combined into orthorectified one day mosaics. The local solar illumination
122 geometry and a digital elevation model (DEM) are applied to compute a terrain illumination model
123 which is applied for radiometric topography correction. After cloud screening, the FSC retrieval
124 method *SCAmod* is applied to the terrain and illumination corrected reflectances for the pixels
125 interpreted as cloud-free. Statistical uncertainty for all cloud-free pixels is also determined. Finally,
126 some thematic masks (e.g. permanent snow and ice/glacier, water, missing/invalid data) are used for
127 final product generation. These procedures are described in more detail in Metsämäki et al., (2014).

128 The processing software, running on a Linux OS-based Bright Beowulf cluster has been written in
129 ANSI C and is operated at the FMI Sodankylä satellite data center, which also houses the data for the
130 user community at (www.globsnow.info).

131 The *Daily Fractional Snow Cover* (DFSC) product provides fractional snow cover in percentage
 132 (%) per grid cell for all satellite overpasses of a given day. If there are multiple snow observations
 133 (only far north within a day), the satellite observations applied are those acquired under the highest
 134 solar elevation. The FSC is provided only for observations at sun zenith angle $< 73^\circ$. The *Weekly*
 135 *Aggregated Fractional Snow Cover* (WFSC) product provides per-pixel FSC from the last available
 136 cloud-free observation within the past seven days. The *Monthly Aggregated Fractional Snow Cover*
 137 (MFSC) product is based on DFSC products for the given calendar month. Fractional Snow Cover is
 138 provided as an average of all available cloud-free estimates within the period. The *Daily 4-classes*
 139 *Snow Cover* (D4FSC) product provides snow cover classified into four categories per grid cell for all
 140 satellite overpasses of a given day. In terms of FSC, the four classes represent:

- 141 • $0\% \leq \text{FSC} \leq 10\%$
- 142 • $10\% < \text{FSC} \leq 50\%$
- 143 • $50\% < \text{FSC} \leq 90\%$
- 144 • $90\% < \text{FSC} \leq 100\%$

145 Weekly and monthly products based on D4FSC are also provided, with same specifications as for
 146 daily products. The dataset is available at <http://www.globsnow.info/se/>. Fig. 1 presents an example
 147 of daily, weekly and monthly SE products for April 2006.



156 Figure 1. A sample set of GlobSnow v2.1 SE products for April 2006. *Top*: daily product 13 April,
 157 *Middle*: weekly product 15 April, *Bottom*: monthly product.

158
159
160
161
162
163
164
165
166
167
168
169
170
171
172
173
174
175
176
177
178
179
180
181
182
183

The GlobSnow SE daily product DFSC is characterized by data gaps due to the narrow swath width of the ATSR-2 and AATSR sensors. This, together with the 3 days revisit time, implies that number of observations used in the development of weekly and monthly composites is limited. This weakens the ability of these products to capture high temporal changes (snow deposited and melted in a period of a few days). This has implications for the feasibility of the products, for instance in climate change studies. However, these issues are not covered by the present paper as the focus is on the daily product.

3. Description of the FSC retrieval method

3.1 SCAMod and additional rules

The semi-empirical reflectance model-based method *SCAMod* originates from the radiative transfer theory and describes the scene reflectance as a mixture of three major constituents – opaque forest canopy, snow and snow-free ground, which are interconnected through the *apparent forest transmissivity* and the snow fraction. Transmissivity, in turn, can be derived from reflectance observations under conditions that highlight the presence of forest canopy – namely in the presence of full snow cover on the ground. Given the transmissivity can be determined with an appropriate accuracy, *SCAMod* enables the consideration of the masking effect of forest canopy in fractional snow cover estimation (Metsämäki et al., 2005, 2012). *SCAMod* was first developed for fractional snow mapping in Finland representing a variety of boreal landscapes including dense evergreen coniferous forests. At the early stage of the GlobSnow-1 project, *SCAMod* was found to also be feasible for hemispheric FSC retrievals, provided the transmissivity can be determined on a hemispheric scale.

SCAMod expresses the observed reflectance as follows:

$$\rho_{\lambda,obs}(FSC) = (1-t_{\lambda}^2) * \rho_{\lambda,forest} + t_{\lambda}^2 * [FSC * \rho_{\lambda,snow} + (1-FSC) * \rho_{\lambda,ground}] , \quad (1)$$

184 where $\rho_{\lambda,snow}$, $\rho_{\lambda,ground}$ and $\rho_{\lambda,forest}$ are generally applicable pre-determined reflectances of (wet) snow,
 185 snow-free ground and forest canopy at wavelength λ , respectively. $\rho_{\lambda,obs}$ stands for the observed
 186 reflectance from the calculation unit area. t_{λ}^2 stands for the apparent two-way transmissivity of the
 187 unit area.

188

189 FSC (range 0–1 here) is solved from (1) as follows:

190

$$191 \quad FSC = \frac{\frac{1}{t_{\lambda}^2} * \rho_{\lambda,obs} + (1 - \frac{1}{t_{\lambda}^2}) * \rho_{\lambda,forest} - \rho_{\lambda,ground}}{\rho_{\lambda,snow} - \rho_{\lambda,ground}}. \quad (2)$$

192

193 In GlobSnow, SCAMod employs top-of-atmosphere reflectance acquisitions of ATSR-2/AATSR
 194 Band 1 (545–565nm) as $\rho_{\lambda,obs}$. The feasible values for the three reflectance constituents are based on
 195 MODIS band 4 (550nm) reflectance observations and field spectroscopy, see section 3.2.
 196 Transmissivity is derived from (1) using reflectance acquisitions from fully snow-covered terrain,
 197 which allows the unknown FSC to be neglected and reduces the equation to a linear interpolation
 198 problem.

199 SCAMod may result in $FSC > 1$ (100%) if the observed reflectance is higher than the maximum
 200 allowed by the model with the applied parameters. This may be due to the non-representative
 201 transmissivity or, more likely, due to a prevailing snow reflectance higher than that applied in the
 202 model. This is the case for dry snow introducing higher reflectance than that of melting (wet) snow,
 203 for example. Likewise, SCAMod may result in $FSC < 0$ if the observed reflectance is lower than the
 204 minimum allowed by the model. Consequently, fractional snow cover is constrained to upper and
 205 lower limits of 100% and 0% respectively.

206 An additional test for identification of snow-free conditions is applied to avoid false snow
 207 detection if the observed reflectance from snow-free terrain is higher than assumed by the model. The
 208 Normalized Difference Snow Index (NDSI, Riggs et al., 1994) is used to identify confident snow-free
 209 cases. Since the NDSI decreases with the decreasing snow fraction (Hall et al., 1995) it is possible to
 210 determine a threshold to identify a snow-free situation. The value 0.4 (or 0.1 for forested areas) as

211 proposed by Klein et al., (1998) however, is not feasible for SCAMod purposes, as the intention is to
212 also identify small snow fractions accurately without thresholding that is too conservative. A
213 threshold of -0.02 is used in GlobSnow:

214 IF NDSI < -0.02 THEN FSC = 0. (3)

215

216 This threshold was empirically derived from NDSI observations from Terra/MODIS imagery over
217 Finland, using weather station data and information on general climatology to verify snow-free
218 conditions soon after snow disappearance. Using a slightly negative value is also supported by
219 findings by e.g. Xin et al., (2012) and Niemi et al., (2012), reporting negative values for dense forest
220 areas particularly with non-nadir view angles. A very low NDSI – although above zero – is also
221 accepted by the MOD10_L2 fractional snow algorithm (Salomonson and Appel, 2006) for very low
222 snow fractions.

223 Temperature screening is applied to avoid false snow identifications caused by highly reflective
224 non-snow targets like certain non-identified cloud types or warm bright mineral surfaces. A pixel is
225 designated ‘snow-free’ if its temperature > threshold. Temperature screening is applied e.g. in the
226 provision of MODIS Collection 5 snow products where a temperature threshold of 283 K is used
227 (Hall et al., 2002; Riggs et al., 2006). Although the temperature screening was later found to cause
228 low snow fractions to ‘disappear’, particularly in rocky mountain areas where snow-free patches may
229 raise the surface temperature above the threshold (Riggs and Hall, 2012), the screening is used in
230 GlobSnow v2.0 and v2.1 SE production. However, to reduce false snow omissions, the threshold was
231 set higher than 283 K; it is based on a single band (band 7, centered at 12 μ m) approximation of the
232 surface brightness temperature:

233 IF temperature > 288 K THEN FSC=0. (4)

234

235 **3.2 SCAMod parameterization**

236 SCAMod uses predetermined values for the three reflectance constituents and for the transmissivity.

237 The success of FSC retrievals therefore depends on the representativeness of these model parameters.

238 Here we present the principles for determination of these; a more detailed description is given in
239 Metsämäki et al., (2014). It should be noted that the parameters have been determined mostly using
240 Terra/MODIS acquisitions. This is because the narrow swath width of the ATSR-2/AATSR
241 drastically reduces the amount of suitable observations while MODIS provides daily global coverage.
242 The ATSR-2/AATSR spectral bands used in GlobSnow SE product generation correspond well to the
243 ones provided by MODIS, so this is considered a reasonable approach.

244

245 **3.2.1 Snow and forest canopy reflectance**

246 The generally applicable value for snow reflectance $\rho_{\lambda, \text{snow}}$ in eq. (1) is empirically derived from i)
247 MODIS band 4 reflectance observations from snow-covered non-forested areas (Metsämäki et al.,
248 2012) and ii) at-ground spectral measurements conducted in Finland (Salminen et al., 2009; Niemi et
249 al., 2012). For the latter, conversion from at-ground reflectance to top-of-atmosphere reflectance was
250 conducted using the Simplified Method for Atmospheric Correction (SMAC) (Rahman and Dedieu
251 (1994); Berthelot, 2003) with the standard atmosphere adjusted to Finnish springtime conditions.

252 It is recognized that using only one value for snow reflectance does not correspond to the large
253 variation in snow reflectance caused by varying grain size, impurities and thickness (e.g. Dozier et al.,
254 2009; Nolin and Dozier, 2000; Painter and Dozier, 2004; Warren; 1982). In the provision of
255 GlobSnow SE, these variances are propagated in the uncertainty of FSC, while the applied constant
256 value ($\rho_{\lambda, \text{snow}}=0.65$) is considered a reasonable approximation for the average case.

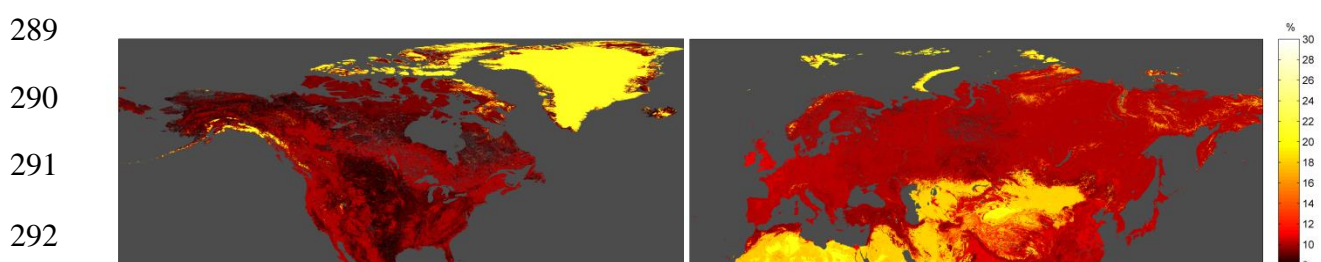
257 Forest canopy reflectance $\rho_{\lambda, \text{forest}}$ in eq. (1) refers to totally opaque forest canopy. Since such
258 canopies are not easy to identify, we have to rely on observations from canopies we assume are close
259 to opaque. The applied value was mainly derived from MODIS reflectance observations from
260 carefully selected very dense boreal forests over Finland and Russia (Metsämäki et al., 2012), but also
261 from reflectance measurement of thick layers of Scots pine branches at laboratory condition (Niemi et
262 al., 2012). A value of 0.08 for $\rho_{\lambda, \text{forest}}$ is considered reasonable for FSC estimation.

263

264 **3.2.2 Snow-free ground reflectance**

265 The earlier GlobSnow v1.2 SE implementation of SCAMod uses a fixed value $\rho_{\lambda,ground} = 10\%$ (0.10)
266 for the visible wavelengths around 555 nm. This value was derived by sampling MODIS top-of-
267 atmosphere reflectances over representative areas as well as from at-ground reflectance measurements
268 with portable spectrometer (Metsämäki et al., 2012; Salminen et al., 2009). In practice, the spatial and
269 temporal variability of $\rho_{\lambda,ground}$ causes an error contribution to FSC estimation. In v2.0 and v2.1 SE
270 production this variability is considered by determination of spatially varying post-winter snow-free
271 ground reflectance map to be applied by SCAMod as auxiliary data. For seasonally snow-covered
272 areas in the Northern Hemisphere, the snow-free ground reflectance statistics were determined using
273 reflectance observations and land cover information (ESA GlobCover, Bicheron et al., 2008) for
274 training areas in Europe and in North America. The observations representing post-melt (assumed
275 mostly wet) snow-free ground were extracted from the MODIS reflectance time-series using
276 methodology by Salminen et al., (2013). The extracted pixel-wise values were then related to the
277 GlobCover data to generate class-stratified snow-free ground reflectance statistics. The swath level
278 MOD02HKM data were calibrated to top-of-atmosphere reflectances and processed into a 0.005°
279 geographical grid.

280 For the majority of the classes, snow-free ground reflectance statistics were derived from the
281 European training area, while for 4 classes, separate analyses were made for North America and
282 Europe. For regions with ephemeral snow, the snow-free ground reflectance statistics were
283 determined by analysing selected MOD09 products for Africa and Asia. MODTRAN atmospheric
284 code (Anderson et al., 1995; Berk et al., 1989) simulations were applied for conversion to top-of-
285 atmosphere reflectances. For the classes that remained not analyzed (e.g. forests), a snow-free ground
286 reflectance of 10% was assigned, based on earlier implementations of SCAMod (Metsämäki et al.,
287 2012). The statistics gained, combined with the GlobCover data, were employed to generate the
288 spatially varying snow-free ground reflectance map, presented in Fig. 2.



293 Figure 2. Snow-free ground reflectance maps applied in the GlobSnow v2.0 and v2.1 SE production:
294 North America (*Left*) and Eurasia (*Right*).

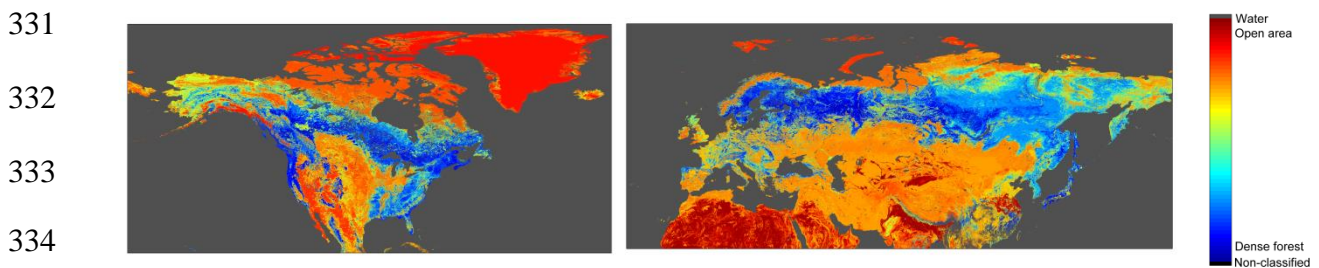
295

296 **3.2.3 Apparent forest transmissivity**

297 The transmissivity for a target area can be established using reflectance data acquired under full snow
298 cover conditions (Metsämäki et al., 2005). At a hemispheric scale, this approach would be very
299 laborious to accomplish; therefore, a new method for generating the transmissivity map using global
300 land cover data too was developed for GlobSnow (Metsämäki et al., 2012). Transmissivity was first
301 determined from MODIS reflectance acquisitions for several extensive 'training areas' in the Northern
302 Hemisphere. For each area, transmissivity statistics (mean and standard deviation) were determined
303 for the present GlobCover classes; these were then combined to obtain class-stratified values. The
304 transmissivity for each 0.01° pixel can be expressed as a linear combination of class-wise average
305 transmissivity and the occurrence of the corresponding classes in that pixel (4×4 GlobCover 0.0025°
306 pixels in one GlobSnow pixel). The feasibility of this approach was verified through evaluating the
307 FSC retrievals against Landsat TM/ETM+ -based FSC and against Finnish *in situ* FSC measurements.
308 These evaluations are presented in detail in Metsämäki et al., (2012).

309 The GlobCover-based transmissivity map was applied in the provision of GlobSnow v1.2 SE
310 products. Although the general performance of this approach was considered good, some
311 underestimations were identified for very dense forests (Solberg et al., 2011). Comparisons between
312 the original MODIS-derived transmissivities and the GlobCover-based transmissivities revealed that
313 the method could not fully capture the densest forests but these were typically assigned with
314 transmissivity that was too high. Further analysis indicated that most problems occurred with four
315 particular boreal forest classes, each class representing dense and moderate canopies. This was seen in
316 the class-stratified transmissivity statistics as high standard deviation. As a result, the average
317 transmissivity gained did not properly represent either of the forest types. Hence it was concluded that
318 the GlobCover-based approach would benefit from external data accounting for the forest density. For
319 this purpose, visible white-sky albedo as provided by ESA GlobAlbedo (Müller et al., 2012) was

320 selected. Although there is an increase in albedo over snow-covered boreal forests (snow on or
321 beneath the canopy), these albedos are clearly lower than those from non-forested areas (Barlage et
322 al., 2005; Moody et al., 2007). The analysis between the albedo from selected wintertime 8-day
323 composites – with snow cover on terrain prevailing – showed that there is a high linear correlation
324 between the albedo and MODIS-derived transmissivity particularly around very low values. Using
325 this linear relationship, transmissivity values for the densest forest were adjusted to be lower than in
326 the original transmissivity map. It should be noted that this technique is valid only in the presence of
327 full snow cover, corresponding to transmissivity calculations as presented in Metsämäki et al., (2005,
328 2012). Therefore, GlobSnow SWE products (Takala et al., 2011) were used to identify the snow-
329 covered areas before launching the correction procedure. The two-way transmissivity map for the
330 Northern Hemisphere is presented in Fig. 3.



335 Figure 3. Map of the apparent two-way forest transmissivity map (t^2) for North America (*Left*) and for
336 Eurasia (*Right*).

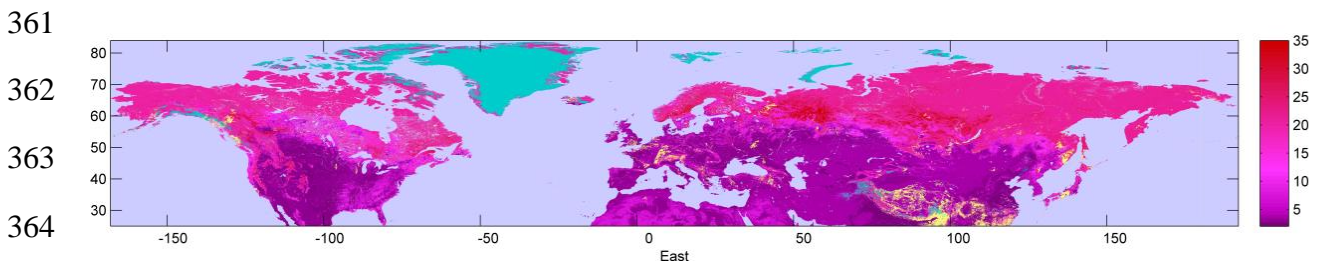
337

338 3.3 Determination of the FSC uncertainty

339 The estimated uncertainty for FSC is provided as a separate layer in SE products. This statistical error
340 accounts for the uncertainty due to the variations in the SCAMod parameters. At the moment, the
341 uncertainty layer does not include systematic error contribution as this would require extensive *in situ*
342 validation work which has not yet been compiled. Hence, the SE uncertainty corresponds to an
343 unbiased standard error of an FSC estimate in %-units (Metsämäki et al., 2014). It is determined by
344 applying an error propagation analysis to the inverted SCAMod reflectance model (Metsämäki et al.,
345 2005; Salminen et al., 2013). The applied error propagation analysis considers the variability of the
346 different factors affecting the satellite-observations in various measurement conditions, these

347 variations being determined during or straight after the snow season. This implies that the uncertainty
348 does not particularly include intra-annual variations – however it does depend on the level of FSC.

349 The relevant error contributors in FSC retrieval with SCAMod are the variabilities in snow
350 reflectance, forest transmissivity, forest canopy reflectance and snow-free ground reflectance. For the
351 transmissivity, these variations are derived from the MODIS top-of-atmosphere reflectances (view
352 zenith angles 0–50° in forward scatter and backscatter directions, sun zenith angles 61–75°)
353 employed in the transmissivity generation for the training area in Europe (Metsämäki et al., 2012).
354 For snow, the standard deviation is derived from at-ground spectral measurements mainly made in
355 Sodankylä, Finland. These measurements were conducted for different grain sizes and depths of the
356 snowpack (Niemi et al., 2012; Salminen et al., 2009). Standard deviations for snow-free ground
357 reflectances are derived from MODIS acquisitions as described in Salminen et al., (2013); the view
358 zenith angles and sun zenith angles ranging as for the transmissivity, depending on the GlobCover
359 class. The uncertainty for monthly product MFSC is calculated as an average of uncertainties of the
360 daily products within the corresponding period; an example for April 2006 is presented in Fig. 4.



365 Figure 4. Uncertainty layer for v2.1 SE Monthly product, April 2006. Statistical error (non-biased
366 standard error) for each FSC estimate is provided in FSC %-units. A yellow color indicates cloudy
367 areas, cyan indicates non-classified areas of permanent snow and ice (see class ‘Glacier’ in Fig. 1),
368 according to the GlobCover data.

369

370 **4. Cloud screening**

371 Several cloud detection methods for optical remote sensing data with particular considerations for
372 snow/cloud discrimination have been developed (e.g. Ackerman et al., 1998; Allen, 1990;
373 Khlopenkov et al., 2007; Knudby et al., 2011; Saunders and Kriebel, 1988). The problem, however,

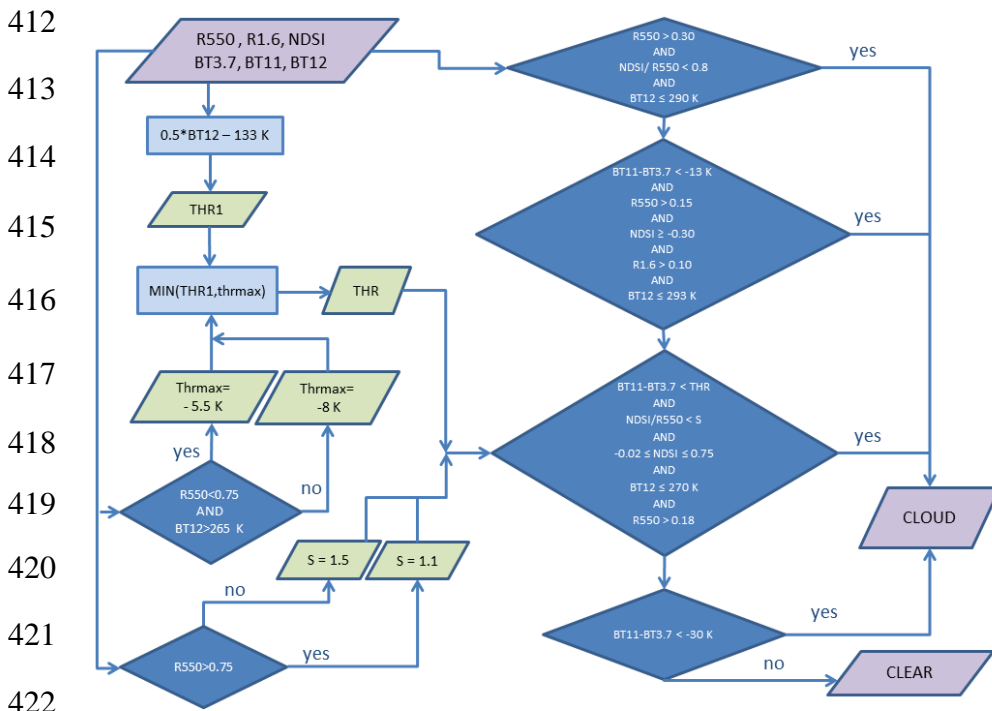
374 has not been completely solved. The cloud/snow confusion causing false cloud commissions at the
375 edges of snow cover in particular may be a problem (Hall and Riggs, 2007; Solberg et al., 2011;
376 Tekeli et al., 2005). Since the AATSR operational cloud mask is reported to have difficulties over
377 snow-covered terrain (e.g. Plummer et al., 2008), a new cloud screening method was established for
378 the generation of the GlobSnow SE v1.2 data record (Metsämäki et al., 2011). A simple and
379 computationally low-cost binary (cloud/clear) classifier method was based on ATSR-2/AATSR data
380 without any external data source was named SCDA (Simple Cloud Detection Algorithm). Based on
381 the evaluations for the GlobSnow SE v1.2 dataset, it was later concluded that improvements for cloud
382 screening were still necessary. Therefore, a new cloud screening method called SCDA2.0, was
383 developed and implemented for the SE v2.0 processing chain. SCDA2.0 was designed to be used for
384 optical and infrared data from sensors such as Terra/MODIS, ERS-2/ATSR-2, ENVISAT/AATSR,
385 NPP Suomi/VIIRS and the future Sentinel-3 SLSTR. The method uses wavelength bands 550 nm, 1.6
386 μm , 3.7 μm , 11 μm and 12 μm , common for these sensors. Fig. 5 presents the cloud screening
387 scheme, with these bands referred to as R550, R1.6, BT3.7, BT11 and BT12, correspondingly.

388 The methodology is based on the several empirically determined decision rules, determined from
389 selected training areas representing (by visual judgement) clouds, snow-covered terrain, partially
390 snow-covered terrain and snow-free terrain. NPP Suomi/VIIRS and Terra/MODIS acquisitions from
391 several dates and from different regions over Northern Hemisphere provided the training data. The
392 decision rules were determined with a heuristic approach by investigating the distributions of features
393 – reflectances, brightness temperatures and their-related ratios – in different projections. Fig. 5
394 presents the cloud screening scheme. It should be noted that the success of cloud screening is based
395 on visual evaluation of several (other than training data) MODIS, VIIRS and AATSR acquisitions, i.e.
396 no *in situ* cloud observations were used for the assessments. Instead, a comparison against the cloud
397 mask provided with the MOD10_L2 fractional snow product was made for several MODIS swaths,
398 particularly for acquisitions made during snow melt period.

399 The development work for SCDA2.0 was intended particularly for identification of clouds
400 throughout potential snow seasons for such regions where snow events are typical. Identification of
401 clouds over regions without even ephemeral snow is therefore not given any left specific attention,

402 which means that thin semi-transparent clouds over areas confidently assumed to be snow-free may
 403 not be classified as cloud. This kind of ‘liberal’ mask would retain more area for snow/non-snow
 404 mapping purposes. As a drawback, some non-detected clouds still may confuse the snow mapping
 405 method, leading to false snow commissions during summer months. In most cases however, non-
 406 detected clouds in summertime images are assigned ‘snow-free’ by the FSC retrieval method.

407 Finally, the original cloud mask is enhanced by expanding by a width of 1–3 pixels. This would
 408 diminish the presence of partly cloud-contaminated pixels at the cloud edges and also removes part of
 409 the shadows cast by clouds. In practice, expansion is carried out by convolving the cloud mask with a
 410 7×5 sliding window which is asymmetrically weighted to expand more to the north-west (shadow
 411 casting) side of the clouds.



423 Figure 5. SCDA2.0 cloud scheme used in GlobSnow v2.0 and v2.1 SE production.

425 5. Considerations for accuracy assessment

426 5.1 Uncertainty originating from the FSC retrieval method

427 The SCAMod reflectance model, when applying several pre-fixed parameters either as spatially
 428 varying or static values, is sensitive to the representativeness of these parameters. For instance, only

429 one generally applicable value for snow reflectance is currently used. Considering snow reflectance
430 varies highly with snow properties e.g. grain size, black carbon (BC) concentration and depth of the
431 snowpack as well as with viewing/illumination conditions, this simplification has implications for the
432 accuracy of FSC retrievals. For instance, the decrease in snow visible albedo (or reflectance) can be
433 close to 40% at very high black carbon concentrations or with a very thin snowpack (Warren, 2013).
434 Ignoring this strong decrease, SCAMod would produce an almost 50% (relative) FSC underestimation
435 compared with what would be gained by applying the decreased ‘true’ value. Similarly, the non-
436 representativeness of snow-free ground reflectance or forest canopy reflectance increases the
437 inaccuracy of FSC retrievals. As described in Section 3.2.2, the snow-free ground reflectance map is
438 based on observations at the time of snow melt-off and therefore does not reflect the seasonal changes
439 in the snow-free ground reflectance. In addition to this, some of the classes were directly assigned a
440 value of 10%. This has potential implications for the accuracy of FSC retrievals. If the true level of
441 local snow free ground reflectance differs from the applied static value, a systematic error (bias) is
442 introduced in FSC retrievals, see Salminen et al., (2013), their Eq. 4 (note that there is a printing error;
443 subtraction of FSC is missing at the end of Eq. 4). The impact of non-representative snow-free
444 ground reflectance is demonstrated in Section 5.3 – case study #3.

445 There are potential inaccuracies originating from the idea of SCAMod’s forest compensation. In
446 hemispheric-scale comparisons against MODIS Collection 5 MOD10_L2 fractional snow products,
447 the GlobSnow project team has found that GlobSnow SE products provide higher FSC for boreal
448 forests than MODIS does. During high snow season this is probably in favor of GlobSnow SE as
449 MODIS seems to underestimate FSC in boreal forests (Metsämäki et al., 2012) while SCAMod shows
450 less underestimation. Yet SCAMod may lead to overestimation of FSC in very dense forests with low
451 transmissivity. This is because at low transmissivity, forest is a relatively dark target with or without
452 under-canopy snow, and the reflectance model allows very limited dynamics for the observed
453 reflectance $\rho_{\lambda,obs}$ (see Eq. 1) in the FSC range of 0–100%. Accordingly, $\rho_{\lambda,obs}$ (FSC=0%) is only a few
454 steps from $\rho_{\lambda,obs}$ (FSC=100%), both being low values. As a consequence, a small increase in

455 reflectance (e.g. by atmospheric aerosols) shows up as a strongly increased FSC estimate. These
456 effects will be evaluated in further hemispheric scale validations and cannot be covered in this paper.

457 FSC retrievals are also sensitive to the representativeness of the local transmissivity. The possible
458 non-representativeness mainly originates from the technique used in the generation of NH
459 transmissivity (see Section 3.2.3): for a certain class, a high standard deviation of the MODIS-
460 derived transmissivities implies that the mean of this distribution is a poor estimate for a class-
461 stratified value. This issue is discussed and demonstrated in Metsämäki et al., (2012), where the
462 impact of using GlobCover-based transmissivity instead of MODIS-derived transmissivity is
463 demonstrated for selected regions in western Eurasia. For these regions however, only a minor
464 decrease in RMSE was found, when FSC retrievals were compared with TM/ETM+ reference FSC.

465 One source of inaccuracy is the misclassification/outdated information in GlobCover, as the
466 transmissivity map and snow-free ground reflectance map are generated using GlobCover to obtain
467 the NH coverage. For instance, a prominent error occurs if GlobCover indicates dense forest for a
468 pixel that is actually forest-free (e.g. after clearcutting which does not show up in GlobCover). In such
469 case, FSC is highly overestimated throughout the season.

470 It should also be noted that the GlobSnow implementation of SCAMod is optimized for springtime
471 (ablation) conditions, which is evident from the way the parameters are determined. This is also
472 emphasized by the applied limitation for the sun zenith angle (max. 73° is accepted) in GlobSnow SE
473 production, which limits the mapped area quite drastically during the late accumulation period and the
474 high snow season in northern latitudes. However this limitation is however not crucial for snow
475 mapping during the melting period in boreal forest and tundra zones and of course has no impact on
476 mid-latitude snow retrieval.

477

478 **5.2 Generation of reference FSC from Landsat TM/ETM+ imagery**

479 Hemispheric-scale snow maps can be evaluated by comparing them to snow information derived from
480 high-resolution imagery, with the assumption that these provide an appropriate approximation of the
481 'truth'. This is in practice the only option as there are only very limited *in situ* data particularly on
482 fractional snow cover are available. It is obvious that the evaluation result strongly depends on the

483 quality of the reference data. When comparing the GlobSnow DFSC to these reference data, we try to
484 i) identify how the comparison reflects the possible inaccuracies of the DFSC and ii) define the
485 conditions where the reference data are not representative.

486 Due to the good availability of Landsat TM/ETM+ data, these have been commonly used for
487 evaluations of coarser resolution snow products (e.g. Metsämäki et al., 2012; Painter et al., 2009;
488 Rittger et al., 2013; Vikhamar and Solberg, 2003). Two methods for reference FSC determination
489 from TM/ETM+ data are investigated here: i) the fractional snow method by Salomonson and Appel,
490 (2006) and ii) the binary snow retrieval method by Klein et al., (1998). These methods provide snow
491 information for high-resolution pixels, and the information can be aggregated into coarse resolution
492 grid to ‘simulate’ the FSC estimates under evaluation. In addition to this, a reasonable candidate for
493 reference FSC generation would be spectral unmixing providing high accuracy data (e.g. Painter et al.
494 2009; Rittger et al. 2013), but due to its more complex implementation spectral unmixing was
495 excluded in this study.

496 The fractional snow retrieval method by Salomonson and Appel (2006), referred to as the
497 *Salomonson and Appel method* hereafter, is based on a statistical linear regression between FSC and
498 the NDSI ($FSC = -0.01 + 1.45 \times NDSI$); determination of globally applicable regression coefficients for
499 computing FSC from the NDSI was carried out using several Landsat TM scenes in different locations
500 in the Northern Hemisphere. This is the baseline method in the MODIS MOD10A1 and MOD10_L2
501 fractional products (Hall et al., 2002; Riggs et al., 2006). From MODIS, this methodology is reported
502 to provide FSC with a mean absolute error of < 10% (Salomonson and Appel, 2004). While using this
503 technique for TM/ETM+ data, we assume that the same accuracy can also be reached with higher
504 resolution data. Although the NDSI regression technique has a weaker performance for dense forest
505 areas than for open or sparsely forested regions because a lower NDSI is observed from forests
506 (Salomonson and Appel, 2004; Metsämäki et al., 2012; Niemi et al., 2012) it was decided here to use
507 this approach uniformly for all TM/ETM+ scenes. However, the presence of forest must be taken into
508 consideration when interpreting the results.

509 The binary snow mapping method by Klein et al., (1998) – referred to as the *Klein method*
510 hereafter – is based on NDSI-thresholding, with additional rules utilizing the NDVI (Normalized

511 Difference Vegetation Index) as well as some reflectance thresholds. This method classifies a pixel as
512 ‘snow’ if its snow fraction is $> \sim 50\%$, the threshold depending on the land cover. After binary
513 mapping in TM/ETM+ nominal resolution, the coarser resolution FSC can be retrieved by averaging
514 the binary data. Although this technique may result in biased FSC, providing underestimations at low
515 snow fractions and overestimations at high snow fractions (Rittger et al., 2013), these data serve as
516 complementary information for our efforts to assess the feasibility of TM/ETM+ data for SE product
517 evaluation. It has also been found to identify snow in forests better than the Salomonson and Appel
518 method (Salomonson and Appel, 2004; Rittger et al., 2013).

519 Overall, the TM/ETM+ processing includes calculation of top-of-atmosphere reflectances for
520 visible and near-infrared band 2 (0.52–0.60 μm), band 3 (0.63–0.69 μm), band 4 (0.76–0.90 μm) and
521 band 5 (1.55–1.75 μm) to provide the NDSI and NDVI, as well as brightness temperature for band 6
522 (10.40–12.50 μm). Band 6 is applied to identify warm surfaces so that whenever the temperature
523 exceeds 288 K, the pixel is assigned as ‘snow-free’ (this is an addition to the Salomonson and Appel
524 method and to the Klein method). Topographic correction is applied to the scenes with varying
525 elevations using the Ekstrand method (Ekstrand, 1996). The data is reprojected and resampled to a
526 0.00025° grid in the WGS-84 system. Then the Salomonson and Appel method or Klein method is
527 applied. These high resolution data are then aggregated to 0.01° pixel size to match the pixel size of
528 the GlobSnow SE product. In this paper, the resulting FSC maps are hereafter referred to as *FSC_{Klein}*
529 and *FSC_{salapp}*. Manually masked clouds and water pixels (according to the GlobCover classification)
530 were excluded in the analysis.

531

532 **5.3 Evaluations of GlobSnow DFSC in case of different land covers**

533 Five Landsat TM/ETM+ scenes were processed for comparison to the GlobSnow DFSC. These scenes
534 were selected to represent different land covers, aiming for preliminary assessment of the product
535 performance in general. In these assessments, the feasibility of the two methods described above for
536 reference data generation is addressed. For two of the scenes, also comparison to the MODIS
537 Collection 5 MOD10_L2 fractional snow product is presented.

538 The differences between estimated and independent reference FSC (N cases) are analyzed using
539 root-mean-squared-error (RMSE) and Bias as validation metrics:

540

$$541 \quad RMSE = \sqrt{\frac{1}{N} \sum (FSC_{estimated} - FSC_{reference})^2} \quad (5)$$

542

$$543 \quad Bias = \frac{1}{N} \sum (FSC_{estimated} - FSC_{reference}) \quad (6)$$

544 where $FSC_{estimated}$ and $FSC_{reference}$ refer to estimated and reference FSC at 0.01° pixel size.

545 When using these metrics, it should be noted that the idea of using aggregated high-resolution snow
546 data (either binary or fractional) to ‘simulate’ coarse resolution FSC includes a certain limitation.
547 Namely, with high-resolution data it is possible to identify snow in just one pixel which then shows
548 up in the aggregated FSC, but which is too little to create enough of a ‘snow’ signal derived from the
549 coarse resolution pixel directly. This means that particularly at low snow fractions but also at higher
550 snow fractions, FSC aggregated from high-resolution FSC is persistently higher than direct coarse
551 resolution FSC (here we assume that the signal from coarse resolution pixel is a linear combination of
552 those from the high-resolution pixels; this approximation should be appropriate in this context). This
553 is a typical way of using high resolution data for validations; however the issue of different scales in
554 FSC retrievals is present regardless of the retrieval method applied.

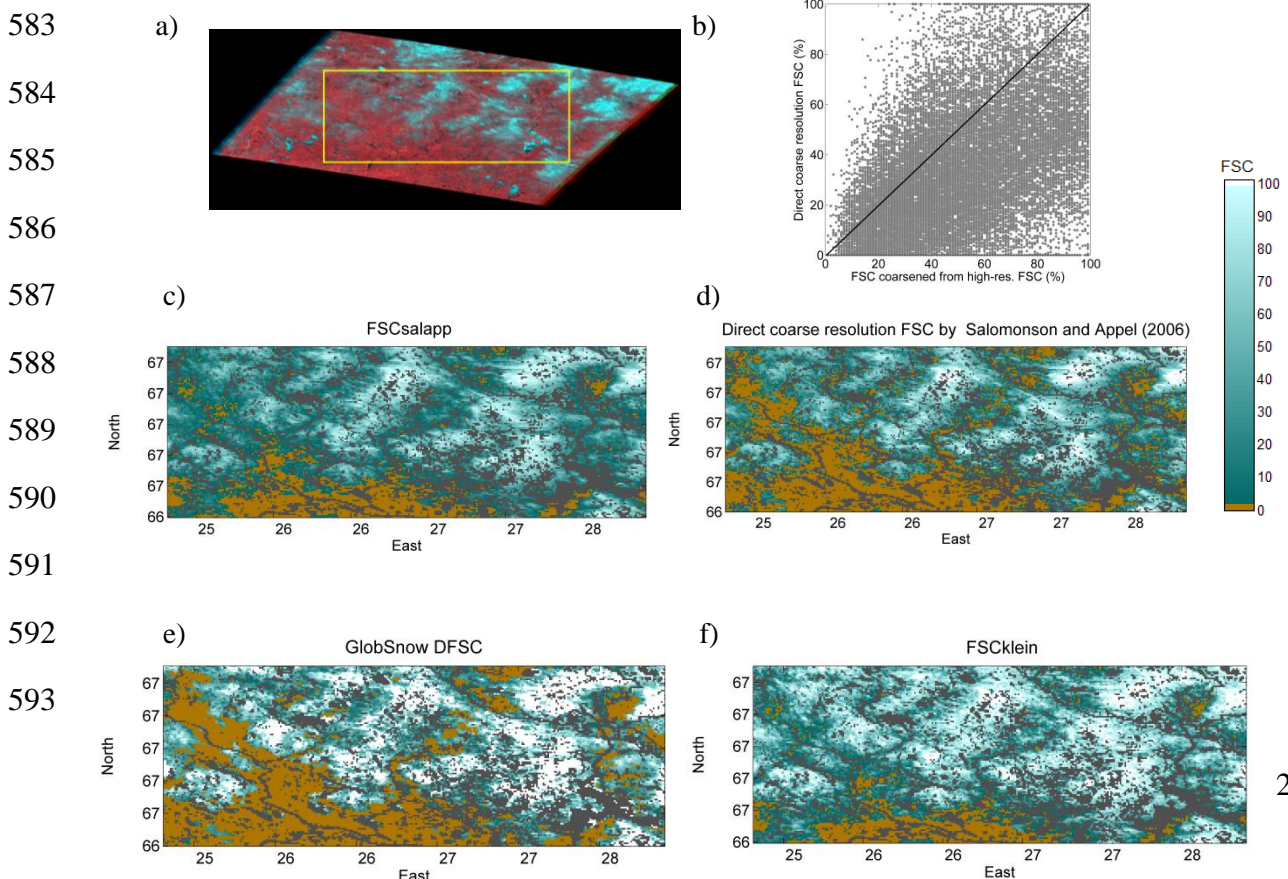
555

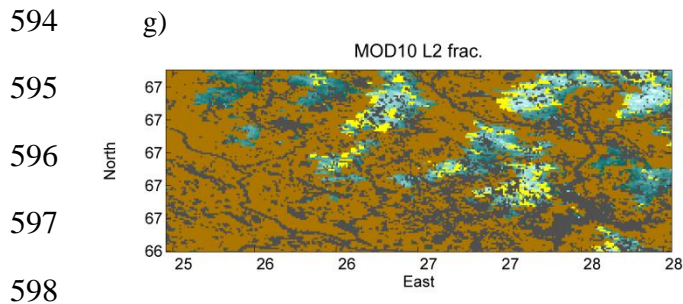
556 ***Case study #1: forested region***

557 The reference FSC generation using different methods is demonstrated for TM scene
558 LT51910132006125KIS00 over Northern Finland, May05 2006, see Fig. 6a (yellow rectangle
559 indicates the area extracted for visualization of the FSC-maps in more detail in Figs. 6c-g). ~80% of
560 the scene area is covered by conifer forests. The 13 weather stations distributed throughout the scene
561 area report snow fractions 0–50% (according to the e-code describing the snow coverage in the range
562 of vision of a human observer); stations are located in open areas so higher snow fractions can be
563 assumed for forests where snow usually stays longer (e.g. Metsämäki et al., 2012). This is highlighted
564 by the fact that a snow depth of 0 cm (punctual measurement) is reported at the majority of the
565 stations, even though at the same time the e-code indicates snow. FSCsalapp (Fig. 6c) shows

566 fractional snow over most of the area, the average scene FSC is 31%. Salomonson and Appel method
 567 applied directly to data coarsened to 0.01° pixel size produces less snow as expected (Fig. 6d); the
 568 average scene FSC is 27%. Both of these for the entire scene are presented in Fig. 6b. From this
 569 simple analysis we can deduce that the differences obtained in the FSC can in principle originate from
 570 different scales, not necessarily from the FSC retrieval method itself. This should be considered when
 571 interpreting the validation results in general.

572 The average scene FSC by FSCKlein (Fig. 6f) is 48%. The GlobSnow SE (Fig. 6e) shows
 573 relatively good correspondence with both TM-based maps but loses some of the low snow fractions,
 574 the average scene FSC is 39%. The fact that the GlobSnow DFSC lies between FSCsalapp and
 575 FSCKlein is expected, as the former tends to underestimate in forests whereas the latter tends to
 576 overestimate. For comparison, the MOD10_L2 fractional snow product is also presented in Fig. 6g. It
 577 does not agree with Fig. 6d although both maps are based on the same method (the MOD10_L2
 578 produced from the Terra/MODIS acquisition on the very same day) but shows much less snow, most
 579 likely due the thermal screen applied after actual FSC retrieval (Riggs et al., 2006). The average scene
 580 FSC from the MOD10_L2 is only 10%. Here the MOD10_L2 also shows the typical false cloud
 581 commissions at the edge of snow-covered areas (yellow color in Fig. 6g), this problem is alleviated in
 582 the GlobSnow DFSC as the SCDA2.0 cloud mask is more liberal.





599 Figure 6. FSC at 0.01° pixel size, for Landsat TM scene area LT51910132006125KIS00, Northern
 600 Finland, on May 05, 2005. a) The entire scene as RGB composite of TM-bands 5, 3 and 2, b) FSC's
 601 based on applying the Salomonson and Appel method to TM data, either through aggregation of high-
 602 resolution pixels (FSCsalapp) or directly to coarsened pixels, c)–d) the corresponding FSC maps, e)
 603 the GlobSnow DFSC, f) FSCklein, g) MOD10_L2 fractional product, the yellow color indicates
 604 clouds.

605

606 ***Case study #2: non-forested region***

607 In the following case study, the GlobSnow DFSC is compared to fractional snow cover maps from
 608 Landsat-5 TM scenes LE71540301999319SGS00 (Kazakhstan, Central Asia, November 15, 1999)
 609 and LT50400151999152PAC00 (Nunavut Canada, June 01, 1999), see Fig. 7. Both scenes are
 610 characterized by fractional snow cover over terrain that was practically non-forested.

611 For the Kazakhstan scene (Fig. 7, top pane) comparison of the GlobSnow DFSC and FSCklein
 612 would first indicate that the GlobSnow DFSC overestimates the low fractions and underestimates the
 613 high snow fractions. However, since FSCklein is typically biased (see above) this would likely be an
 614 erroneous interpretation. Indeed, comparison with FSCsalapp shows a better correspondence with an
 615 RMSE of 11% and correlation coefficient of 0.94, compared to that of FSCklein (RMSE 15%,
 616 correlation coefficient 0.89). It is also likely that the snow-free ground reflectance employed by
 617 SCAMod is relatively representative for the Kazakhstan scene, as at low snow fractions no noticeable
 618 bias is found. However, the GlobSnow DFSC shows a slightly lower FSC than FSCsalapp, which
 619 agrees with the above discussed issue of using different scales in FSC retrieval, see Fig. 6b.

620 For the Nunavut scene (Fig. 7, bottom pane), the comparison between the GlobSnow DFSC and
 621 TM-based FSC's shows good agreement, resulting in an RSME of 13% for FSCklein and FSCsalapp.

622 The correlation coefficients for FSCklein and FSCsalapp are 0.93 and 0.94, respectively. It is likely
 623 that the snow-free ground reflectance applied is not as representative as for the Kazakhstan scene, as
 624 low snow fractions are overestimated. Overestimation occurs if the snow-free ground reflectance
 625 applied is lower than truly present in the target area. This issue is discussed later in case study #3.

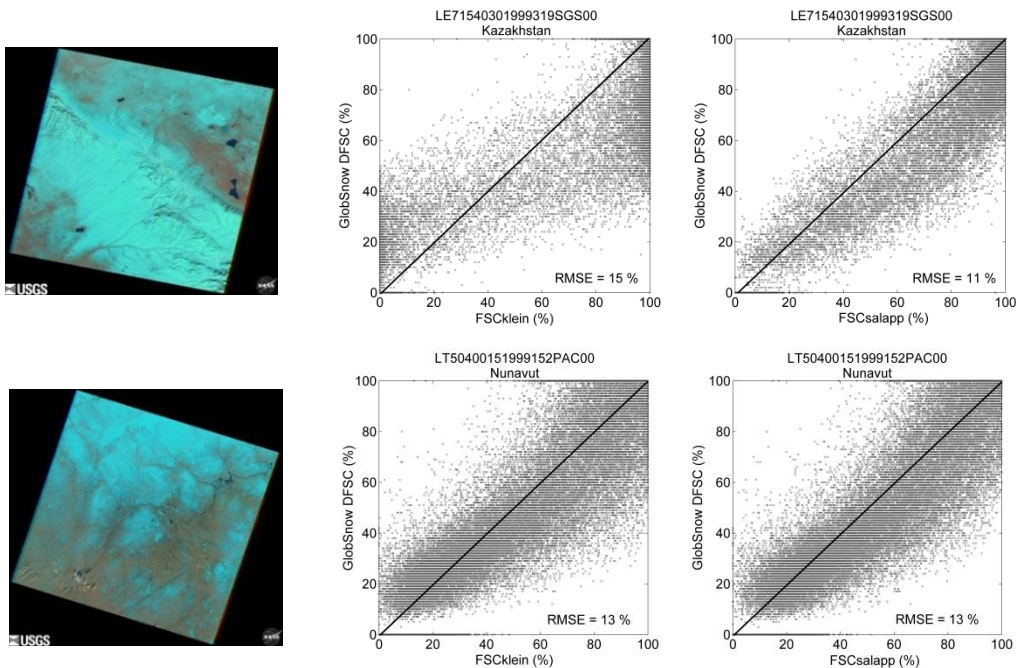
626

627

628

629

630



631

632

633

634

635

636 Figure 7. Comparison between the GlobSnow DFSC and two methods for FSC retrieval from
 637 TM/ETM+ data over Kazakhstan (top pane) and Nunavut, Canada (bottom pane). *Left:* Browse
 638 image, *Middle:* FSCklein, *Right:* FSCsalapp.

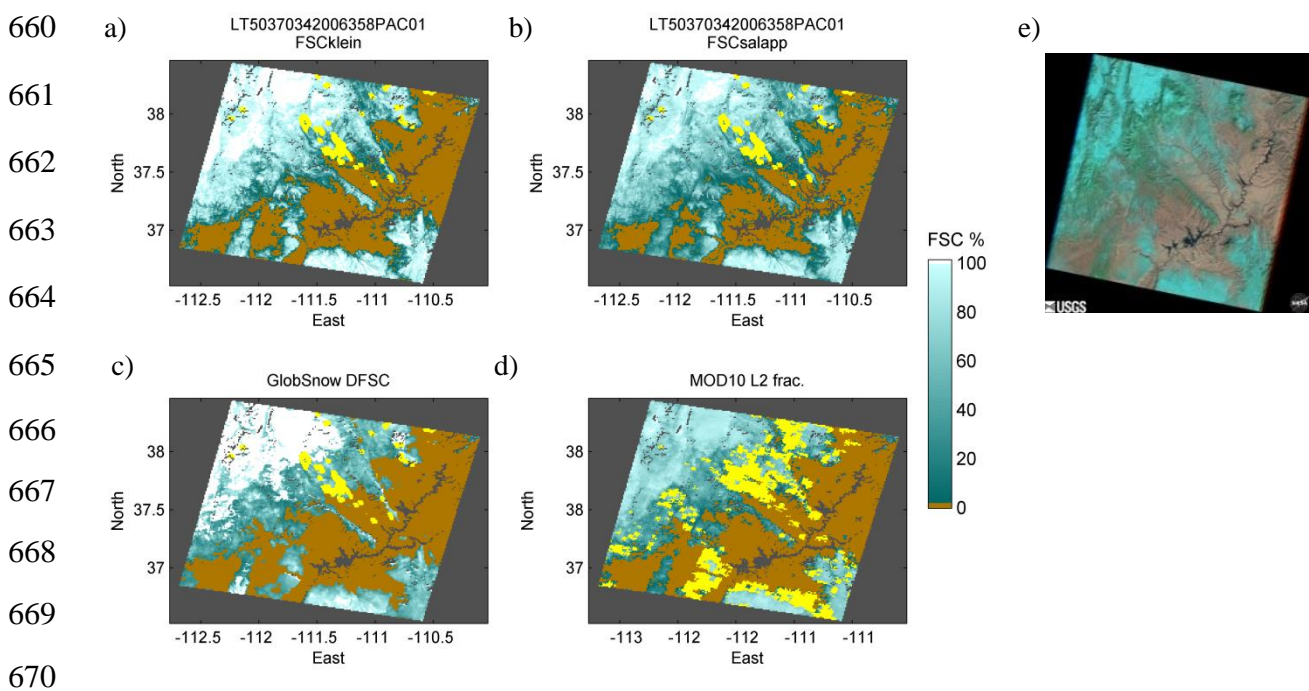
639

640 ***Case study #3: non-forested region with considerations for snow-free ground reflectance***

641 In the following case study, the effect of the non-representative value of snow-free ground
 642 reflectance on the FSC estimation is demonstrated for TM scene LT5037342006358PAC01 over
 643 Utah, on December 24, 2006, see Fig. 8e. The early evaluation of the GlobSnow v2.0 and v2.1 DFSC
 644 products indicates that a systematic error (overestimation) is evident for areas of class 130 ('closed to
 645 open shrubland' according to GlobCover data) in Western US, where this prevalent class represents
 646 sparsely vegetated and semiarid areas in intermontane plateaus. The value of 10% was assigned to this
 647 class in the snow-free ground reflectance map. Analysis of local reflectances in the TM scene
 648 indicates that the south-eastern part of the scene is characterized by a reflectance level significantly

649 higher than 10% in snow-free conditions. This would lead to FSC overestimation when applying
 650 SCAMod. The DFSC, FSCklein and FSCsalapp are presented in Fig. 8; for comparison, fractional
 651 snow provided by the MOD10_L2 for the same day is also presented. Generally, all products show
 652 the same spatial distribution for snow. Indeed, the probable overestimation is present in the DFSC as
 653 high snow fractions are pronounced, while MOD10_L2 seems to provide a lower FSC than the other
 654 three products.

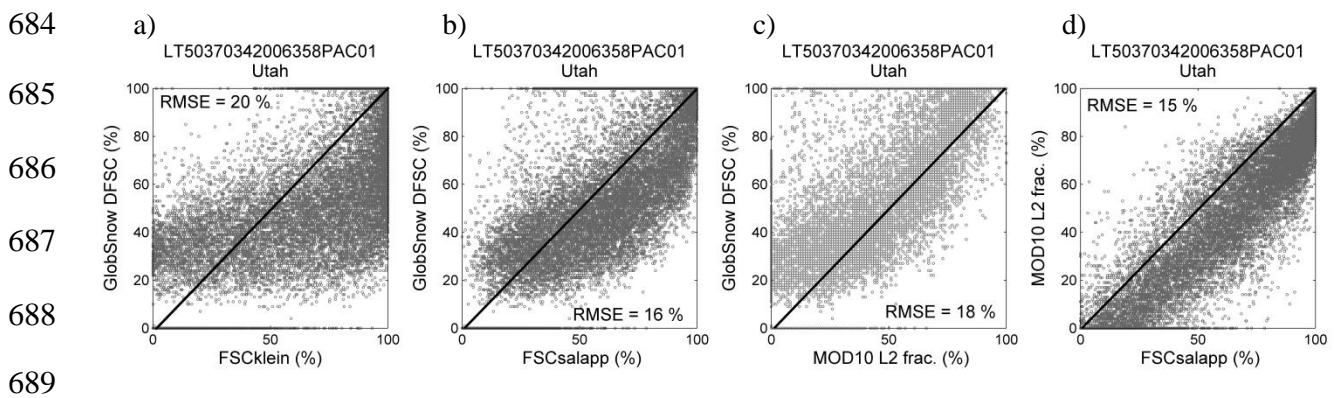
655 Incidentally, Fig. 8 shows the better performance of the SCDA2.0 cloud screening method for this
 656 particular scene. The typical problem of false cloud commissions at the edge of snow-covered terrain
 657 (see Section 4) is visible in the MOD10_L2 product, as shown by extensive areas of yellow color. The
 658 corresponding cloud mask by SCDA2.0 is clearly lesser in the area, shown in yellow color in the
 659 GlobSnow DFSC product and also in TM-based FSC maps.



671 Figure 8. Fractional snow cover maps as provided by a) FSCklein, b) FSCsalapp, c) the GlobSnow
 672 DFSC, d) MOD10_L2, for TM scene LT5037342006358PAC01 over Utah, US, on December 24,
 673 2006 (e). The yellow color corresponds to clouds.

674 The differences between the four products stand out in pixel by pixel comparisons in Fig. 9. Again,
 675 FSCklein results in a higher RMSE (20%) than FSCsalapp (16%) when compared with the DFSC.
 676

677 The very likely overestimation particularly at low snow fractions in the DFSC (see above) is also
 678 pronounced in Fig. 9a and 9b as the DFSC practically loses all snow fractions between 0–15%.
 679 Comparison between the DFSC and MOD10_L2 (Fig. 9c) indicates relatively good correspondance
 680 with an RMSE of 18% and correlation coefficient of 0.92, except again for low snow fractions.
 681 Finally, the RMSE for MOD10_L2 when compared with FSCsalapp is 15% (Fig. 9d), again
 682 demonstrating the scale problem discussed in 5.2, but having a high correlation of 0.96 which is
 683 expected as both are based on the same method.



690 Figure 9. The GlobSnow v2.1 DFSC compared with fractional snow provided by a) FSCklein, b)
 691 FSCsalapp, c) MOD10_L2, for TM scene area LT5037342006358PAC01 over Utah, US, on
 692 December 24, 2006. d) MOD10_L2 and FSCsalapp for the same scene area.

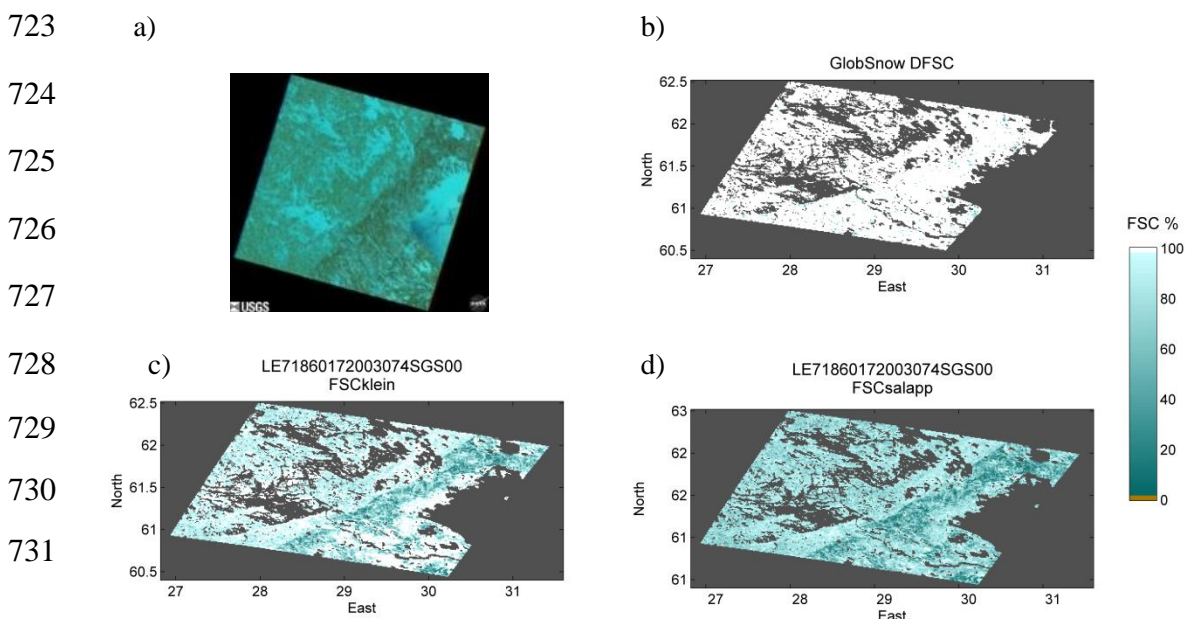
693

694 ***Case study #4: very dense forest canopy***

695 Forest canopy partly masks the view from satellite sensor to the ground, which typically leads to
 696 inaccuracies in fractional snow cover estimation. In GlobSnow SE products, the canopy obscurance
 697 is compensated for through SCAMod, but evaluation of the success of the methodology is somewhat
 698 difficult due to the lack of appropriate reference data. The TM/ETM+ -based methods described
 699 above are not very suitable for forested areas. The Klein method basically identifies the snow in forest
 700 through the NDSI-thresholding, but overestimates the moderate to high snow fractions while
 701 underestimating or even missing the low snow fractions. The Salomonson and Appel method
 702 responds better to the different fractions through linear regression but leads to underestimation as a
 703 snow-covered forest provides a lower NDSI than a snow-covered non-forest area.

704 Here we demonstrate the performance of FSC_{klein} and FSC_{salapp} for ETM+ scene
 705 LE71860172003074SGS00 over the Finnish-Russian border on March 15, 2003, Fig. 10a. From
 706 Finnish *in situ* observations at several weather stations and from general climatology we know that the
 707 scene area is fully snow-covered. The area is characterized by numerous lakes (ice covered at the time
 708 of the image acquisition) and by dense to very dense boreal forests (the latter indicated by the bluish
 709 area across the scene from the north-east corner towards the south-west). Since the very dense forests
 710 even with under-canopy snow have ETM+ band 2 reflectance below 10%, the reflectance
 711 thresholding applied in the provision of FSC_{klein} and FSC_{salapp} results in FSC=0 for many of the
 712 forest pixels. So it is evident that the reflectance thresholding is not reasonable for the densest forests.
 713 As expected, FSC_{klein} (Fig. 10c) succeeds relatively well in identifying full snow cover, except for
 714 the densest forest (yet underestimating, average scene FSC is 88%), while FSC_{salapp} (Fig. 10d)
 715 results in slight underestimations all over the scene (average scene FSC is 74%). Hence, in this case
 716 we can consider FSC_{klein} to better represent the ‘truth’.

717 The GlobSnow DFSC, from the previous date as no concurrent AATSR acquisition was available,
 718 performs well with an average scene FSC of 99%, see Fig. 10b. However, the RMSE’s gained from
 719 pixel-to-pixel comparison with FSC_{klein} and FSC_{salapp} are as high as 21% and 31%, respectively.
 720 This analysis indicates that for densely forested areas, neither of the TM/ETM+ -based methods can
 721 provide a reliable reference, and statistical metrics like the RMSE or correlation coefficient are only
 722 suggestive.



732

733 Figure 10. a) ETM+ scene LE71860172003074SGS00, March15, 2003, over the Finnish-Russian
734 borderline with dense forests, full snow cover prevailing, b) the GlobSnow DFSC, c) FSCklein, d)
735 FSCsalapp. The dark grey color indicates no-data (outside image acquisition or water pixels).

736

737 From the above results, one might deduce that the Klein method would be preferred over the
738 Salomonson and Appel method for generating the reference FSC for forests. However the result only
739 concerns forests with full snow cover. For fractional snow, the Klein method tends to overestimate,
740 except for low snow fractions for which it tends to underestimate. The level of FSC at which snow
741 overestimation turns into underestimation varies according to forest density i.e. scene to scene but is
742 clearly below 50% according to Rittger et al., (2013). So the Klein method would be reasonable only
743 to identify the presence of snow in forests, not the snow fraction. As the Salomonson and Appel
744 method is capable of detecting snow in forests as well (although underestimating), it could be
745 recommended in general, particularly as it seems work better for open areas.

746

747 **6. Conclusions**

748 This paper introduces the Snow Extent (SE) product portfolio provided within thr ESA DUE
749 GlobSnow, with special focus on the Daily Fractional Snow Cover (DFSC) of the SE version 2.0
750 released in 2013 and its successor version 2.1 released in 2014. The SE products include hemispheric
751 daily, weekly and monthly maps of Fractional snow cover derived from ERS-2/ATSR-2 and
752 Envisat/AATSR data, spanning 17 years (1995–2012). The fractional snow cover retrieval is based on
753 the SCAMod method relying on a semi-empirical reflectance model. The model parameterization is
754 the key issue for the performance of the method; therefore, the generation of each parameter is
755 summarily described. The method applied in cloud screening is also introduced, with some
756 considerations concerning on its general performance but without going into details.

757 The first evaluations of GlobSnow DFSC are presented along with considerations concerning
758 future validations, including the discussion of issues already noticed. The evaluation experiment is
759 accomplished by comparing the DFSC to high-resolution data-based reference FSC. Actual validation

760 is not presented; instead, the feasibility of two methods for generating the reference FSC from Landsat
761 TM/ETM+ data are investigated for different landcovers, with a particular interest in forested areas.
762 Methods by Klein et al. (1998) and Salomonson and Appel (2006) were tested for five Landsat scene
763 areas. It was concluded that for forests, validation against TM/ETM+ -derived FSC is very easily
764 distorted by the non-representativeness of these reference data. Accordingly, validation results for
765 heavily forested areas can only be suggestive. For sparsely forested and non-forested areas, the
766 fractional snow retrieval methodology by Salomonson and Appel (2006) was found to be more
767 feasible. A likely case of applying a value too low for one of the SCAMod parameters (snow-free
768 ground reflectance) is identified in the US intermontane plateau area. This is well distinguished as
769 overestimated low snow fractions in the DFSC. Some overestimations in very dense forests are also
770 expected, due to the narrow dynamics of reflectance observed from forests, either snow-free or snow-
771 covered. Overall, these first evaluations suggest that GlobSnow SE products give a good performance
772 for forested areas but this is necessarily not shown in validation due to the non-representativeness of
773 the reference data.

774 For two of the scenes investigated, MODIS Collection 5 MOD10_L2 fractional product was also
775 presented and compared with reference data and the GlobSnow DFSC. The analysis of a forested
776 scene indicated that the temperature screening applied in the MOD10_L2 provision would lead to
777 false snow omissions which were not present in the GlobSnow DFSC due to the more liberal
778 temperature screening applied. This also emphasises the advantage of the exclusion of temperature
779 screening in the MODIS Collection 6 snow products. Moreover, snow/cloud confusion present in
780 MOD10_L2 was not identified in the GlobSnow DFSC in the two scenes investigated. However these
781 results are based on limited data; more investigations on the performance of the cloud screening as
782 well as temperature thresholding will be conducted in the future.

783 The results and considerations presented in this paper will be reflected in upcoming studies. There
784 is extensive validation and evaluation work going on within the GlobSnow-2 project, aiming at
785 publication in 2015. The GlobSnow v2.1 SE product is also one of the data sets investigated in the
786 ESA funded project SnowPEX (2014–2016, ESA Contract No. 4000111278/14/ILG), where

787 hemispheric-scale evaluation and intercomparison of several Earth observation-based snow products
788 will be carried out.

789

790 **7. Acknowledgements**

791 This paper is based on the work carried out within European Space Agency projects GlobSnow-1 and
792 GlobSnow-2. In particular, the authors would like to thank ESA project officers Bojan Bojkov and
793 Simon Pinnock for their support. We also wish to thank the four anonymous reviewers for their
794 criticism and suggestions that helped in improving the manuscript.

795

796 **References**

797 Ackerman, S., Strabala, K., Menzel, P., Frey, R., Moeller, C. & Gumley, L. (1998). Discriminating
798 clear sky from clouds with MODIS, *Journal of Geophysical Research*, 103(24), 32141–32157.

799

800 Allen, R. C., Jr., Durkee, P. A. & Wash, C. H. (1990). Snow/cloud discrimination with multispectral
801 satellite measurements. *Journal of Applied Meteorology*, 29, 994–1004.

802

803 Anderson, G.P., Kneizys, F. X., Chetwynd, J. H., Wang, J., Hoke, M. L., Rothman, L.S., Kimball,
804 L.M. & McClatchey, R.A. (1995). FASCOD/TRAN/LOWTRAN Past/Present/Future,
805 *Proceedings of the 18th annual Review Conference on Atmospheric Transmission Models*, 06–08 June
806 1995.

807

808 Ault, T. W., Czajkowski, K. P., Benko, T., Coss, J., Struble, J., Spongberg, A., Templin, M. & Gross,
809 C. (2006). Validation of the MODIS snow product and cloud mask using student and NWS
810 cooperative station observations in the Lower Great Lakes Region. *Remote Sensing of Environment*,
811 105, 341–353.

812

813 Barlage, M., Zeng, X., Wei, H. & Mitchell, K. (2005). A global 0.05° maximum albedo dataset of
814 snow-covered land based on MODIS observations. *Geophysical Research Letters*, 32, 17.
815

816 Berk, A., Bernstein, L.S. & Robertson, D.C. (1989). MODTRAN: a moderate resolution model for
817 LOWTRAN7, GLTR-89- 0122, Air Force Geophys. Lab., Hanscom AFB, MA, 38pp.
818

819 Berthelot, B. (2003). Coefficients SMAC pour MSG. Tech. rep., Noveltis Internal Report NOV-3066-
820 NT-834.
821

822 Bicheron, P., Defourny, P., Brockmann, C., Schouten, L., Vancutsem, C., Huc, M., Bontemps, S.,
823 Leroy, M., Achard, F., Herold, M., Ranera, F. & Arino, O. (2008). *GLOBCOVER Products*
824 *Description and Validation Report*. Medias France, Toulouse, France. Available at:
825 [http://due.esrin.esa.int/globcover/LandCover_V2.2/GLOBCOVER_Products_Description_Validation](http://due.esrin.esa.int/globcover/LandCover_V2.2/GLOBCOVER_Products_Description_Validation_Report_I2.1.pdf)
826 [_Report_I2.1.pdf](http://due.esrin.esa.int/globcover/LandCover_V2.2/GLOBCOVER_Products_Description_Validation_Report_I2.1.pdf)
827

828 Choi, G., Robinson, D. A. & Kang, S. (2010). Changing Northern Hemisphere Snow
829 Seasons. *Journal of Climate*, 23, 5305–5310.
830

831 Dietz, A. J., Kuenzer, C., Gessner, U. & Dech, S. (2012). Remote sensing of snow – a review of
832 available methods, *International Journal of Remote Sensing*, 33:13, 4094–4134.
833

834 Dozier, J., Green, R., Nolin, A. & Painter, T. (2009). Interpretation of snow properties from imaging
835 spectrometry. *Remote sensing of Environment*, 113, 25–37.
836

837 Ekstrand, S. (1996). Landsat TM-based forest damage assessment: correction for topographic effects.
838 *Photogrammetric Engineering and Remote Sensing*, 62, 151–161.
839

840 Frei, A., Tedesco, M., Lee, S., Foster, J., Hall, D. K., Kelly, R. & Robinson, D. A. (2012). A review
841 of global satellite-derived snow products. *Advances in Space Research*, 50(8), 1007–1029.
842

843 Gong, G., Cohen, J., Entekhabi, D. & Ge, Y. (2007). Hemispheric-scale climate response to Northern
844 Eurasia land surface characteristics and snow anomalies. *Global and Planetary Change*, 56, 359–370.
845

846 Hall, D. K., Riggs, G. A. & Salomonson, V. V. (1995). Development of methods for mapping global
847 snow cover using moderate resolution imaging spectroradiometer data. *Remote Sensing of*
848 *Environment*, 54, 127–140.
849

850 Hall, D. K., Riggs, G. A., Salomonson, V. V., DiGirolamo, N. E. & Bayr, K. J. (2002). MODIS snow-
851 cover products. *Remote sensing of Environment*, 83, 181–194.
852

853 Hall, D. K. & Riggs, G. A. (2007). Accuracy assessment of the MODIS snow products. *Hydrological*
854 *Processes*, 21(12), 1534–1547.
855

856 Huang, X., Liang, T., Zhang, X. & Guo, Z. (2011). Validation of MODIS snow cover products using
857 Landsat and ground measurements during the 2001-2005 snow seasons over northern Xinjiang,
858 China, *International Journal of Remote Sensing*, 32(1), 133–152.
859

860 Khlopenkov, K. V. & Trishchenko, A. P. (2007). SPARC: New cloud, snow, and cloud shadow
861 detection scheme for historical 1-km AVHRR data over Canada. *Journal of Atmospheric and Oceanic*
862 *Technology*, 24(3), 322–343.
863

864 Kite, G. & Pietroniro, A. (1996). Remote sensing applications in hydrological modeling.
865 *Hydrological Sciences Journal*, 41, 563–591.
866

867 Klein, A. G., Hall, D. K. & Riggs, G. A. (1998). Improving snow-cover mapping in forests

868 through the use of a canopy reflectance model. *Hydrological Processes*, 12, 1723–1744.

869

870 Knudby A., Latifovic, R. & Pouliot, D. (2011). A cloud detection algorithm for AATSR data,
871 optimized for daytime observations in Canada. *Remote sensing of Environment*, 115, 3153–3164.

872

873 Metsämäki, S., Anttila, S., Huttunen, M., Vepsäläinen, J. (2005). A feasible method for fractional
874 snow cover mapping in boreal zone based on a reflectance model. *Remote Sensing of Environment*,
875 95, 77–95.

876

877 Metsämäki, S., Mattila, O.-P., Pulliainen, J., Niemi, K., Luojus, K. & Böttcher, K. (2012). An optical
878 reflectance model-based method for fractional snow cover mapping applicable to continental scale.
879 *Remote Sensing of Environment*, 123, 508–521.

880

881 Metsämäki, S., Salminen, M., Pulliainen, J., Luojus, K., Nagler, T., Bippus, G., Solberg, R., Salberg,
882 A.-B., Trier, O. D. & Wiesmann, A. (2014). Algorithm Theoretical Basis Document - SE-algorithm,
883 GlobSnow-2 Deliverable-9 . Available at: http://www.globsnow.info/docs/GS2_SE_ATBD.pdf

884

885 Metsämäki, S., Sandner, R., Nagler, T., Solberg, R., Wangenstein, B., Luojus, K. & Pulliainen, J.
886 (2011). Cloud Detection Algorithm SCDA. *GlobSnow Technical Note 2, European Space Agency*.
887 Available at: http://www.globsnow.info/docs/GlobSnow_technical_note2_scda_final_release.pdf

888

889 Moody, E. G., King, M. D., Schaaf, C. B. & Hall, D. K. (2007). Northern Hemisphere fiveyear
890 average (2000–2004) spectral albedos of surfaces in the presence of snow: Statistics computed from
891 Terra MODIS land products. *Remote Sensing of Environment*, 111, 337–345.

892

893 Müller, J.-P., López, G., Watson, G., Shane, N., Kennedy, T., Yuen, P., Lewis, P., Fischer, J. et al.,
894 (2012). The ESA GlobAlbedo Project for mapping the Earth's land surface albedo for 15 Years from
895 European Sensors. *Proceedings of IGARSS 2012, Munich, Germany, 22–27 June, 2012*.

896

897 Niemi, K., Metsämäki, S., Pulliainen, J., Suokanerva, H., Böttcher, K., Leppäranta, M., Pellikka, P.

898 (2012). The behaviour of mast-borne spectra in a snow-covered boreal forest. *Remote Sensing of*

899 *Environment*, 124, 551-563.

900

901 Nolin, A. W. & Dozier, J. (2000). A hyperspectral method for remotely sensing the grain size of

902 snow. *Remote Sensing of Environment*, 74, 207–216.

903

904 Painter, T. H. & Dozier, J. (2004). Measurements of the hemispherical–directional reflectance of

905 snow at fine spectral and angular resolution. *Journal of Geophysical Research-Atmospheres*, 109,

906 D18.

907

908 Painter, T. H., Rittger, K., McKenzie, C., Slaughter, P., Davis, R. E. & Dozier, J. (2009). Retrieval of

909 subpixel snow covered area, grain size, and albedo from MODIS. *Remote Sensing of Environment*,

910 113, 868–879.

911

912 Plummer, S. (2008). The GLOBCARBON Cloud Detection System for the Along-Track Scanning

913 Radiometer ATSR Sensor Series. *IEEE Transactions on Geoscience and Remote Sensing* 46(6),1718–

914 1727.

915

916 Rahman, H. & Dedieu, G. (1994). SMAC: a simplified method for the atmospheric correction of

917 satellite measurements in the solar spectrum. *International Journal of Remote Sensing*, 15, 123–143.

918

919 Riggs, G. A., Hall, D. K. & Salomonson, V. V. (1994). A snow index for the Landsat Thematic

920 Mapper and Moderate Resolution Imaging Spectroradiometer. *Proceedings of IGARSS 1994*,

921 Pasadena, California, USA, 8–12 August 1994 (pp. 1942–1944).

922

923 Riggs, G. A., Hall, D. K. & Salomonson, V. V. (2006). *MODIS Snow Products User Guide to*
924 *Collection 5*. Available at: http://nsidc.org/data/docs/daac/modis_v5/dorothy_snow_doc.pdf

925 Riggs, G. A. & Hall, D. K. (2012). Improved snow mapping accuracy with revised MODIS snow
926 algorithm. *Proceedings of the 69th Annual Eastern Snow Conference*.

927

928 Rittger, K., Painter, T. H. & Dozier, J. (2013). Assessment of methods for mapping snow cover from
929 MODIS. *Advances in Water Resources*, 51, 367–380.

930

931 Salminen, M., Pulliainen, J., Metsämäki, S., Kontu, A. & Suokanerva, H. (2009).
932 The behaviour of snow and snow-free surface reflectance in boreal forests: Implications to the
933 performance of snow covered area monitoring. *Remote Sensing of Environment*, 113, 907–918.

934

935 Salminen, M., Pulliainen, J., Metsämäki, S., Böttcher, K. & Heinilä, K. (2013). MODIS-derived
936 snow-free ground reflectance statistics of selected Eurasian non-forested land cover types for the
937 application of estimating fractional snow cover. *Remote Sensing of Environment*, 138, 51–64.

938

939 Salomonson, V. V. & Appel, I. (2004). Estimating fractional snow cover from MODIS using the
940 normalized difference snow index. *Remote Sensing of Environment*, 89, 351–360.

941

942 Salomonson, V. V. & Appel, I. (2006). Development of the Aqua MODIS NDSI fractional snow
943 cover algorithm and validation results. *IEEE Transactions on Geoscience and Remote Sensing*, 44,
944 1747–1756.

945

946 Saunders, R. W. & Kriebel, K.T. (1988). An improved method for detecting clear sky and cloudy
947 radiances from AVHRR data. *International Journal of Remote Sensing*, 9(1), 123–150.

948

949 Schmugge, T. J., Kustas, W. P., Ritchie, J., Jackson, T. & Rango, A. (2002). Remote sensing

950 in hydrology. *Advances in Water Resources*, 25, 1367–1385.

951

952 Solberg R. & Andersen, T. (1994). An automatic system for operational snow-cover monitoring in the
953 Norwegian mountain regions. *Proceedings of IGARSS 1994*, Pasadena, California, USA, 8-12 August
954 1994 (pp. 2084–2086).

955

956 Solberg, R., Amlien, J. & Koren, H. (2006). *A review of optical snow cover algorithms*. Norwegian
957 Computing Center Note, no. SAMBA/40/06.

958

959 Solberg, R., Wangensteen, B., Rudjord, Ø., Metsämäki, S., Nagler, T., Sandner, R., Müller, F., Rott,
960 H., Wiesmann, A., Luojus, K., Kangwa, M. & Pulliainen, J. (2011). *Globsnow Snow Extent Product*
961 *Guide. Product Version 1.2*, European Space Agency.

962 Available at: www.globsnow.info/se/GlobSnow_SE_product_readme_v1.2.pdf

963

964 Takala, M., Luojus, K., Pulliainen, J., Derksen, C., Lemmetyinen, J., Kärnä, J. P. & Koskinen, J.
965 (2011). Estimating northern hemisphere snow water equivalent for climate research through
966 assimilation of space-borne radiometer data and ground-based measurements. *Remote Sensing of*
967 *Environment*, 115, 3517–3529.

968

969 Tekeli, E., Akyurek, Z., Sorman, A. A., Sensoy, A. & Sorman, A. U. (2005). Using MODIS Snow
970 Cover Maps in Modeling Snowmelt Runoff Process in the Eastern Part of Turkey. *Remote Sensing of*
971 *Environment*, 97, 216–230.

972

973 Vikhamar, D. & Solberg, R. (2003). Snow-cover mapping in forests by constrained linear spectral
974 unmixing of MODIS data. *Remote Sensing of Environment*, 88, 309–323.

975

976 Wang, X., Xie, H. & Lian, T. (2008). Evaluation of MODIS snow cover and cloud mask and its
977 application in Northern Xinjiang, China. *Remote Sensing of Environment*, 112, 1497–1513.

978

979 Warren, S. G. (1982). Optical properties of snow. *Reviews of Geophysics and Space Physics*, 20, 67–
980 89.

981

982 Warren, S. G. (2013). Can black carbon in snow be detected by remote sensing? *Journal of*
983 *Geophysical Research: Atmospheres*, 118, 779–786.

984

985 Xin, Q. C., Woodcock, C. E., Liu, J. C., Tan, B., Melloh, R. A. & Davis, R. E. (2012). View angle
986 effects on MODIS snow mapping in forests. *Remote Sensing of Environment*, 118, 50–59.

987

988

989 List of figure captions

990

991 Figure 1. A sample set of GlobSnow v2.1 SE products for April 2006. *Top*: daily product 13 April,
992 *Middle*: weekly product 15 April, *Bottom*: monthly product.

993

994 Figure 2. Snow-free ground reflectance maps applied in the GlobSnow v2.0 and v2.1 SE production:
995 North America (*Left*) and Eurasia (*Right*).

996

997 Figure 3. Map of the apparent two-way forest transmissivity map (t^2) for North America (*Left*) and for
998 Eurasia (*Right*).

999

1000 Figure 4. Uncertainty layer for v2.1 SE Monthly product, April 2006. Statistical error (non-biased
1001 standard error) for each FSC estimate is provided in FSC %-units. A yellow color indicates cloudy
1002 areas, cyan indicates non-classified areas of permanent snow and ice (see class ‘Glacier’ in Fig. 1),
1003 according to the GlobCover data.

1004

1005 Figure 5. SCDA2.0 cloud scheme used in GlobSnow v2.0 and v2.1 SE production.

1006

1007 Figure 6. FSC at 0.01° pixel size, for Landsat TM scene area LT51910132006125KIS00, Northern
1008 Finland, on May05 2005. a) The entire scene as RGB composite of TM-bands 5, 3 and 2, b) FSC’s
1009 based on applying the Salomonson and Appel method to TM data, either through aggregation of high-
1010 resolution pixels (FSCsalapp) or directly to coarsened pixels, c)–d) the corresponding FSC maps, e)
1011 GlobSnow DFSC, f) FSCklein, g) MOD10_L2 fractional product, the yellow color indicates clouds.

1012

1013 Figure 7. Comparison between the GlobSnow DFSC and two methods for FSC retrieval from
1014 TM/ETM+ data over Kazakhstan (top pane) and Nunavut, Canada (bottom pane). *Left*: Browse
1015 image, *Middle*: FSCklein, *Right*: FSCsalapp.

1016

1017 Figure 8. Fractional snow cover maps as provided by a) FSCklein, b) FSCsalapp, c) the GlobSnow
1018 DFSC, d) MOD10_L2, for TM scene LT5037342006358PAC01 over Utah, US, on December 24,
1019 2006 (e). The yellow color corresponds to clouds.

1020

1021 Figure 9. The GlobSnow v2.1 DFSC compared with fractional snow provided by a) FSCklein, b)
1022 FSCsalapp, c) MOD10_L2, for TM scene area LT5037342006358PAC01 over Utah, US, on
1023 December 24, 2006. d) MOD10_L2 and FSCsalapp for the same scene area.

1024

1025 Figure 10. a) ETM+ scene LE71860172003074SGS00, March15, 2003, over the Finnish-Russian
1026 borderline with dense forests, full snow cover prevailing, b) the GlobSnow DFSC, c) FSCklein, d)
1027 FSCsalapp. The dark grey color indicates no-data (outside image acquisition or water pixels).

1028

1029